Whole Brain Functional Connectivity Predicted by Indirect Structural Connections

Rasmus Røge*, Karen Sandø Ambrosen*, Kristoffer Jon Albers*, Casper Tabassum Eriksen*,
Matthew George Liptrot*, Mikkel N. Schmidt*, Kristoffer Hougaard Madsen*†, Morten Mørup*
*Department of Applied Mathematics and Computer Science, Technical University of Denmark, Lyngby, Denmark
†Danish Research Centre for Magnetic Resonance, Copenhagen University Hospital Hvidovre, Hvidovre, Denmark

***Abstract*—Modern functional and diffusion magnetic resonance imaging (fMRI and dMRI) provide data from which macro-scale networks of functional and structural whole brain connectivity can be estimated. Although networks derived from these two modalities describe different properties of the human brain, they emerge from the same underlying brain organization, and functional communication is presumably mediated by structural connections. In this paper, we assess the structure-function relationship by evaluating how well functional connectivity can be predicted from structural graphs. Using high-resolution whole brain networks generated with varying density, we contrast the performance of several non-parametric link predictors that measure structural communication flow. While functional connectivity is not well predicted directly by structural connections, we show that superior predictions can be achieved by taking indirect structural pathways into account. In particular, we find that the length of the shortest structural path between brain regions is a good predictor of functional connectivity in sparse networks (density less than one percent), and that this improvement comes from integrating indirect pathways comprising up to three steps. Our results support the existence of important indirect relationships between structure and function, extending beyond the immediate direct structural connections that are typically investigated.**

I. INTRODUCTION

During the last decade there has been a tremendous increase in the obtainable quality of neuroimaging data. Through the efforts of major neuroimaging projects, such as the Human Connectome Project (HCP) [20], to collect and publish large datasets of high resolution data it is now possible to obtain macro-scale whole brain networks of both structural and functional connectivity.

Structural connectivity (SC) in the brain can be estimated in vivo by applying tractography to diffusion magnetic resonance imaging (dMRI) data. Whilst dMRI estimates the directional diffusivity of water molecules in and around neuronal tissue, tractography estimates SC by integrating these resultant voxel-wise proxies of neuronal fibre directions into streamlines which map inter-voxel connections, and subsequently inter-regional connectivity. The result is compactly represented as an adjacency matrix, or graph, with each entry containing the number of streamlines found connecting any two specified regions. These end-point regions are usually chosen to be anatomically-relevant sub-divisions of the cortical gray matter.

Functional connectivity (FC) can also be represented as a connectivity matrix derived from functional magnetic resonance imaging (fMRI) that estimates brain activity using the proxy of blood oxygenation-level dependent (BOLD) signal produced by fMRI sequences. Brain regions that exhibit strong correlation in their BOLD response over the time course of the experiment are considered to be functionally connected, and therefore contain larger values in their respective entries in the FC adjacency matrix.

Even though structural networks derived from dMRI are different from functional networks derived from fMRI, it is a common assumption that the individual processing units of the brain are reflected in both modalities. The first study of this kind, by Koch et al., directly compared FC and SC within a limited spatial domain, specifically neighbouring gyri within a single image slice [13]. Although it only found weak agreement between the two modalities, subsequent studies have shown that SC reflects FC, at least to some extent [9], [17]. However, whilst some studies have suggested that FC is correlated with the strength of direct anatomical connections between cortical regions [12], functional connections have also been observed between regions without direct connections [13], [21], [16], [12]. This suggests that functional correlations may be mediated by structural connections that are not normally accounted for in SC assessment. Whilst there exists the possibility that some structural connections are unrepresented, it is most likely that such functional connections are mediated by multi-step (indirect) structural connections. Indeed, short SC paths (≤ 5 steps) have been shown to explain most of the functional network, demonstrated by the average prediction quality saturating for SC paths of length five [2].

To investigate the extent that such indirect pathways within the SC graph can explain FC, we herein assess the ability of well-established link prediction measures to predict FC graphs from SC graphs. In particular, we assess prediction as a function of the number of steps over which the SC graph is integrated.

Nearly all studies that aim to assess the correspondence between SC and FC do so at a macro-scale, sub-dividing the cortex into large regions, usually pre-defined according to an atlas [10], [6], [2], [7], or by sub-divisions thereof [10], [11]. In 2008, Skudlarski et al. increased the region count to 5000 [16]. Until now, no studies have employed a finer regional division of the cortex. Herein we use a high resolution cortical surface mesh, containing approximately 59,000 vertices in total, with an approximate inter-vertex distance of 2 mm. Furthermore, a few studies comparing SC and FC are restricted to specific

sub-networks, such as the default mode network (DMN) of resting state fMRI, and subsequently only investigate the SC between the activated FC regions [9], [19]. However, these analyses have also been extended to comparison of whole-brain cortical connectivity of fMRI and dMRI [16], [10], [12], [7], and this is also the approach used herein.

For generation of the SC graphs, there is currently no consensus on how the connection "strength" should be estimated. Options here include average FA value along the connection pathways [2], number of streamline counts between endpoints [11], [2], [7], and the physical connection length [11]. All can be viewed as heuristic proxies for connection strength, and as such suffer from the lack of any validation with a gold-standard. The alternative, employed herein, is to avoid any attempt to generate such a proxy measure by thresholding the graph, removing those connections deemed to be noise.

In summary, we herein test the hypothesis that there is an underlying structure-function relationship that can be better modelled by the incorporation of indirect, or multi-step, pathways through the structural graph. Specifically, we quantify measures, from network science link prediction, of communication flow within the structural graph and use these to assess how the number of traversals taken within the structural graph affects its ability to predict the functional graph.

II. DATA AND METHODS

Structural and functional brain connectivity networks were obtained for 25 subjects from the Human Connectome Project (HCP) database (https://ida.loni.usc.edu/login.jsp) using the approximately 59,000 vertices on the cortical surface. The high quality DWI data, acquired by the HCP [20], permits advanced tensor reconstruction models and subsequent tractography methods. Structural brain connectivity graphs were derived from diffusion magnetic resonance imaging (dMRI) data by modeling the local diffusion using FSL's BedpostX for multi-shell data [4] and performing probabilistic tractography using FSL's Probtrackx2 [4], [3]. 1000 streamlines were initiated in each WM voxel and a count added to the connectivity graph if a streamline reached two vertices on the WM surface. The functional graphs were estimated by averaging the Pearson correlation matrices for the left-right and right-left encoding of each of the two sessions of resting state fMRI. Both the functional and structural graphs were binarized by thresholding the raw streamline count graphs at densities of 0.5, 1, 2, and 4 pct. and randomly removing an appropriate number of ties to achieve the exact density.

To predict the fMRI graph from the dMRI graph of the same subject, the list of well-established non-parametric link prediction measures [14], [5], [15] presented in Table I were computed for each dMRI graph and used to predict the fMRI graph as evaluated by the area under curve (AUC) of the receiver operator characteristic (ROC) curve, see also [5], [15]. *Preferential attachment* describes communication as being a product of how much the nodes connect in general (i.e. their degree). *Shortest path* considers communication in terms of step length, incorporating the idea that functional communication is related to the integration of multiple steps in the structural graph, such that regions connected by short paths are more likely to be functionally connected. The remaining methods are based on common neighbors using different weighting schemes. *Common neighbor* quantifies shared structural connections, thus assuming that regions that share structural connections to other regions are more likely to be functionally connected. The *Jaccard* score weights the number of shared structural connections by the number of possible connections, whereas *Adamic/Adar* and *Resource Allocation* put emphasis on neighbors that only have a few structural connections, weighting importance as a function of the neighbors' degree. Finally, *Hub Depressed*, *Hub Promoted* and *Salton* use the degree of the two considered nodes to weight the importance of common neighbors.

Method (abbreviation)	Score s_{ij}
Preferential Attachment (pre)	$d_i d_j$
Shortest Path (sho)	$1/\text{ShortestPath}(\boldsymbol{A}, i, j)$
Common Neighbor (com)	$\sum_t A_{it}A_{jt}$
Jaccard (jac)	$\sum_t A_{it}A_{jt}/(J - \sum_t (1-A_{it})(1-A_{jt}))$
Adamic/Adar (ada)	$\sum_t A_{it}A_{jt}/\log(d_t)$
Resource Allocation (res)	$\sum_t A_{it}A_{jt}/d_t$
Hub Depressed (hbd)	$\sum_t A_{it}A_{jt}/\max(d_i, d_j)$
Hub Promoted (hbp)	$\sum_t A_{it}A_{jt}/\min(d_i, d_j)$
Salton (sal)	$\sum_t A_{it}A_{jt}/\sqrt{d_i d_j}$

TABLE I: Examined link-prediction measures. $\text{ShortestPath}(\boldsymbol{A}, i, j)$ gives the shortest path in graph $\boldsymbol{A}$ between nodes i and j. We consider binary graphs, where $A_{ij} = 1$ when a link exist between i and j, such that $d_i = \sum_j A_{ij}$ is the degree of node i.

III. RESULTS

Fig. 1 shows the performance of all the considered non-parametric link predictors for the four thresholds of graph density. Preferential attachment is consistently found to be the worst performing predictor. All measures based on common neighbor produce similar results for all considered network densities. This is to be expected as these measures are defined by different normalizations of the same property. Shortest path (SP) clearly outperforms the other predictors at the 0.5% threshold. However, as the threshold increases, the SP exhibits a more rapid decrease than the other methods and performs poorer than the common neighbor derived measures at the 2% and 4% thresholds. We attribute this to almost all regions of the networks of 2% and 4% density being connected when considering paths of length up to three, as shown in Fig. 3.

At the 0.5% threshold the number of connections in the graph is relatively sparse. Here the SP outperforms the other metrics. Unlike the other metrics, it is able to consider more than two steps, which suggests that there is information beyond common neighbors constituting paths of step-length two. Using the ROC curve from the shortest path prediction it is possible to calculate the SP AUC limiting the length of considered paths. This is illustrated in the left panel in Fig. 2.

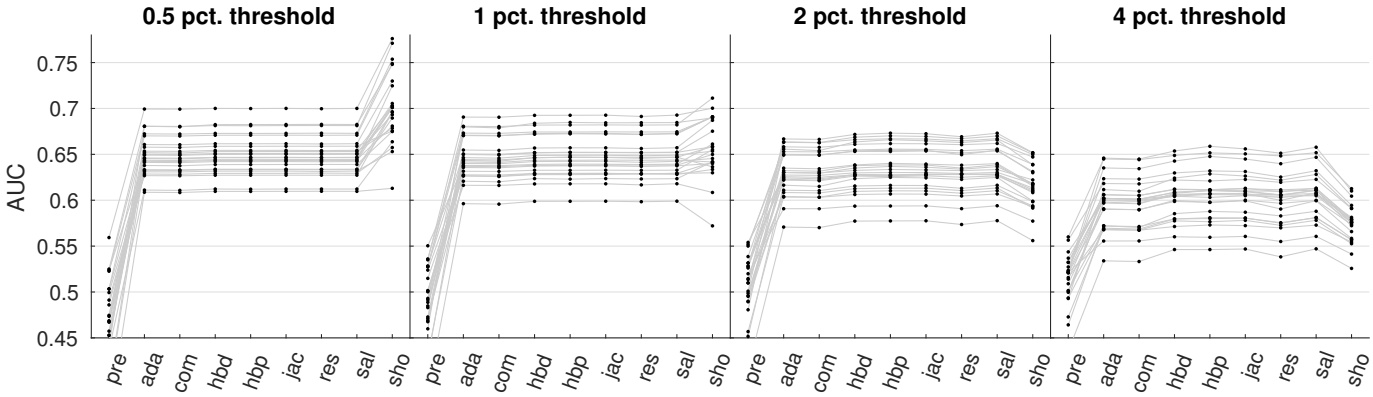

Fig. 1: AUC scores predicting functional connectivity graphs from structural connecitivity graphs for each of the 25 considered subjects and four link-densities of the graphs. The abbreviations for the link predictors are given in Table I.

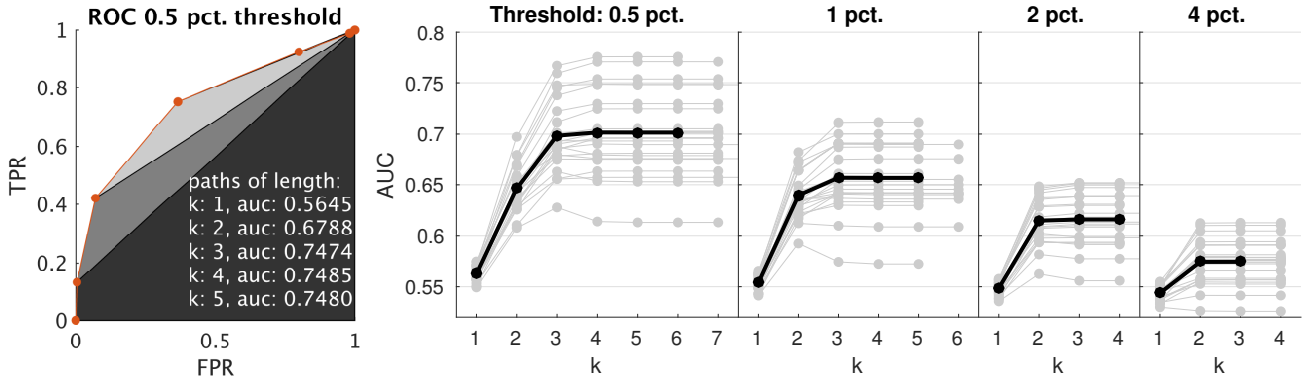

Fig. 2: In the left panel we illustrate the method of computing the truncated shortest path from the shortest path ROC curve. In the right panel we show the truncated shortest path at different path lengths and threshold densities. The shortest path prediction is dominated by links of length two and three, with highest predictive score at three. Note that the AUC score for $k = 1$ is given by the prediction of the functional graph by the raw structural graph.

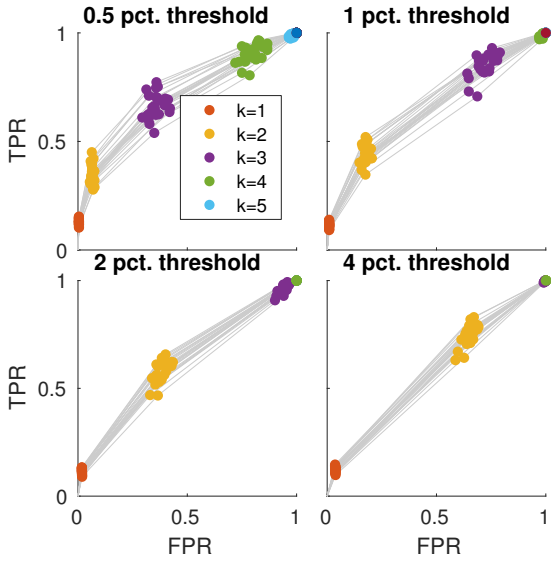

Fig. 3: The ROC curves from the truncated shortest path for the different graph densities.

Even though the SP is able to consider all steplengths (up to full connectivity), Fig. 2 shows that for the 0.5% and 1% thresholds the performance saturates after three steps, and after 2 steps at higher thresholds, see also Fig. 3. This shows that functional connectivity is not the result of direct structural communication between regions (i.e., k=1) but characterized by the integration of a limited number of steps in the SC graph.

IV. DISCUSSION

We investigated different non-parametric link predictor performance in predicting functional connectivity from structural connectivity using high-resolution networks based on data from the HCP project. We found that preferential attachment and direct structural connections (k=1) performed significantly worse for all graph thresholds indicating that functional connectivity is not well accounted for as a product of communication between structural regions of high degree or by direct communication (i.e, the structural adjancency matrix itself). The best performance was achieved with intermediate connections and by taking into consideration the number of common neighbors and the length of the shortest structural communication path. At low densities the integration of up to

three steps improved on the prediction of functional connections. However, we found that incorporating additional steps did not further improve the characterization of FC.

Our results support previous findings that the strength of functional connections decreases with the length of the shortest path [8]. The work by [16] employed weighted graphs (number of streamlines) which may lead to different contrasts within the graphs. Nevertheless they show, in agreement with the results reported herein, that correlation between SC and FC increased for path lengths up to three before decreasing again. In contrast Becker et al. [2] found that the average prediction quality saturates for SC paths of length five. They also used unthresholded weighted graphs (average FA value and streamline counts) and compared correlation between SC and FC. However, they also employed a lower resolution graph, via the AAL parcellation [18], though excluding cerebellum and vermis, resulting in 90 regions. Furthermore, their study included the sub-cortical voxels for both SC and FC, whose anatomical functions often include so-called relay stations which could explain the larger number of steps. Thus, future studies should investigate the effect of sub-cortical regions.

Adachi et al. [1] show that FC is influenced by the network-level cortical architecture and not solely by short anatomical connections (anatomical connections were estimated using tracers). This indicates more complicated communication patterns than serial connected nodes, as investigated in this study using shortest path link prediction. Also, in [8], different properties of the nodes besides the shortest path are investigated. These properties include node degree and path transitivity. They find that node degree along a path (search information) and path transitivity along a path (local detours) better predict FC than using path length alone. This indicates that the global network architecture (and not only the shortest path) influence how well FC can be predicted by SC. Future work should thus consider more advanced predictors that take multiple properties of the SC graph into account.

ACKNOWLEDGMENT

This project was supported by the Lundbeck Foundation (grant no. R105-9813). A Tesla K40, used for processing the structural graphs, was donated by the NVIDIA Corporation. The MRI data used in this work were obtained from the MGH-USC Human Connectome Project (HCP) database (https://ida.loni.usc.edu/login.jsp) in the "500 subjects" release. The HCP project (Principal Investigators: Bruce Rosen, M.D., Ph.D., Martinos Center at Massachusetts General Hospital; Arthur W. Toga, Ph.D., University of California, Los Angeles, Van J. Weeden, MD, Martinos Center at Massachusetts General Hospital) is supported by the National Institute of Dental and Craniofacial Research (NIDCR), the National Institute of Mental Health (NIMH) and the National Institute of Neurological Disorders and Stroke (NINDS). Collectively, the HCP is the result of efforts of co-investigators from the University of California, Los Angeles, Martinos Center for Biomedical Imaging at Massachusetts General Hospital (MGH), Washington University, and the University of Minnesota.

REFERENCES

[1] Y. Adachi, T. Osada, O. Sporns, T. Watanabe, T. Matsui, K. Miyamoto, and Y. Miyashita. Functional connectivity between anatomically unconnected areas is shaped by collective network-level effects in the macaque cortex. *Cerebral cortex*, page bhr234, 2011.

[2] C. O. Becker, S. Pequito, G. J. Pappas, M. B. Miller, S. T. Grafton, D. S. Bassett, and V. M. Preciado. Accurately predicting functional connectivity from diffusion imaging. *arXiv preprint arXiv:1512.02602*, 2015.

[3] T. Behrens, H. J. Berg, S. Jbabdi, M. Rushworth, and M. Woolrich. Probabilistic diffusion tractography with multiple fibre orientations: What can we gain? *Neuroimage*, 34(1):144–155, 2007.

[4] T. Behrens, M. Woolrich, M. Jenkinson, H. Johansen-Berg, R. Nunes, S. Clare, P. Matthews, J. Brady, and S. Smith. Characterization and propagation of uncertainty in diffusion-weighted mr imaging. *Magnetic resonance in medicine*, 50(5):1077–1088, 2003.

[5] A. Clauset, C. Moore, and M. E. Newman. Hierarchical structure and the prediction of missing links in networks. *Nature*, 453(7191):98–101, 2008.

[6] F. Deligianni, G. Varoquaux, B. Thirion, E. Robinson, D. J. Sharp, A. D. Edwards, and D. Rueckert. Relating brain functional connectivity to anatomical connections: Model selection. In *Machine Learning and Interpretation in Neuroimaging*, pages 178–185. Springer, 2012.

[7] P. Garcés, E. Pereda, J. A. Hernández-Tamames, F. Del-Pozo, F. Maestú, and J. Ángel Pineda-Pardo. Multimodal description of whole brain connectivity: A comparison of resting state meg, fmri, and dwi. *Human brain mapping*, 37(1):20–34, 2016.

[8] J. Goñi, M. P. van den Heuvel, A. Avena-Koenigsberger, N. V. de Mendizabal, R. F. Betzel, A. Griffa, P. Hagmann, B. Corominas-Murtra, J.-P. Thiran, and O. Sporns. Resting-brain functional connectivity predicted by analytic measures of network communication. *Proceedings of the National Academy of Sciences*, 111(2):833–838, 2014.

[9] M. D. Greicius, K. Supekar, V. Menon, and R. F. Dougherty. Resting-state functional connectivity reflects structural connectivity in the default mode network. *Cerebral cortex*, 19(1):72–78, 2009.

[10] P. Hagmann, L. Cammoun, X. Gigandet, R. Meuli, C. J. Honey, V. J. Wedeen, and O. Sporns. Mapping the structural core of human cerebral cortex. *PLoS biology*, 6(7):e159, 2008.

[11] A. M. Hermundstad, D. S. Bassett, K. S. Brown, E. M. Aminoff, D. Clewett, S. Freeman, A. Frithsen, A. Johnson, C. M. Tipper, M. B. Miller, et al. Structural foundations of resting-state and task-based functional connectivity in the human brain. *Proceedings of the National Academy of Sciences*, 110(15):6169–6174, 2013.

[12] C. Honey, O. Sporns, L. Cammoun, X. Gigandet, J.-P. Thiran, R. Meuli, and P. Hagmann. Predicting human resting-state functional connectivity from structural connectivity. *Proceedings of the National Academy of Sciences*, 106(6):2035–2040, 2009.

[13] M. A. Koch, D. G. Norris, and M. Hund-Georgiadis. An investigation of functional and anatomical connectivity using magnetic resonance imaging. *Neuroimage*, 16(1):241–250, 2002.

[14] D. Liben-Nowell and J. Kleinberg. The link-prediction problem for social networks. *Journal of the American society for information science and technology*, 58(7):1019–1031, 2007.

[15] L. Lü and T. Zhou. Link prediction in complex networks: A survey. *Physica A: Statistical Mechanics and its Applications*, 390(6):1150–1170, 2011.

[16] P. Skudlarski, K. Jagannathan, V. D. Calhoun, M. Hampson, B. A. Skudlarska, and G. Pearlson. Measuring brain connectivity: diffusion tensor imaging validates resting state temporal correlations. *Neuroimage*, 43(3):554–561, 2008.

[17] O. Sporns. Contributions and challenges for network models in cognitive neuroscience. *Nature neuroscience*, 17(5):652–660, 2014.

[18] N. Tzourio-Mazoyer, B. Landeau, D. Papathanassiou, F. Crivello, O. Etard, N. Delcroix, B. Mazoyer, and M. Joliot. Automated anatomical labeling of activations in spm using a macroscopic anatomical parcellation of the mni mri single-subject brain. *Neuroimage*, 15(1):273–289, 2002.

[19] M. P. Van Den Heuvel, R. C. Mandl, R. S. Kahn, H. Pol, and E. Hilleke. Functionally linked resting-state networks reflect the underlying structural connectivity architecture of the human brain. *Human brain mapping*, 30(10):3127–3141, 2009.

[20] D. C. Van Essen, S. M. Smith, D. M. Barch, T. E. Behrens, E. Yacoub, and K. Ugurbil. The wu-minn human connectome project: an overview. *Neuroimage*, 80:62–79, 2013.

[21] J. L. Vincent, G. H. Patel, M. D. Fox, A. Z. Snyder, J. T. Baker, D. C. Van Essen, J. M. Zempel, L. H. Snyder, M. Corbetta, and M. E. Raichle. Intrinsic functional architecture in the anaesthetized monkey brain. *Nature*, 447(7140):83–86, 2007.